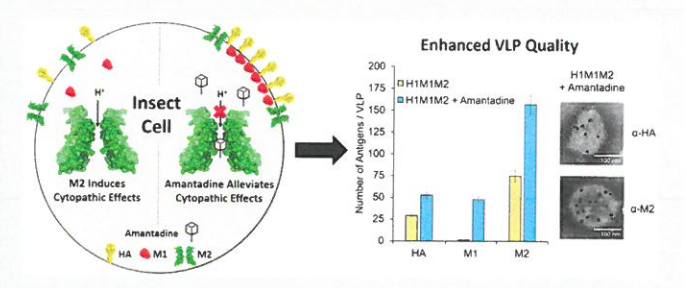
Andrew J. Zak, Brett D. Hill, Syed M. Rizvi, Mason R. Smith, Madeleine Yang, and Fei Wen\*

Department of Chemical Engineering, University of Michigan, Ann Arbor, Michigan 48109, United States

Supporting Information

See https://pubs.acs.org/sharingguidelines for options on how to legitimately share published articles

ABSTRACT: To provide broader protection and eliminate the need for annual update of influenza vaccines, biomolecular engineering of influenza virus-like particles (VLPs) to display more conserved influenza proteins such as the matrix protein M2 has been explored. However, achieving high surface density of full-length M2 in influenza VLPs has been left unrealized. In this study, we show that the ion channel activity of M2 induces significant cytopathic effects in Spodoptera frugiperda (Sf9) insect cells when expressed using M2encoding baculovirus. These effects include altered Sf9 cell



morphology and reduced baculovirus replication, resulting in impaired influenza protein expression and thus VLP production. On the basis of the function of M2, we hypothesized that blocking its ion channel activity could potentially relieve these cytopathic effects, and thus restore influenza protein expression to improve VLP production. The use of the M2 inhibitor amantadine indeed improves Sf9 cellular expression not only of M2 (~3-fold), but also of hemagglutinin (HA) (~7-fold) and of matrix protein M1 (~3-fold) when coexpressed to produce influenza VLPs. This increased cellular expression of all three influenza proteins further leads to ~2-fold greater VLP yield. More importantly, the quality of the resulting influenza VLPs is significantly improved, as demonstrated by the ~2-fold, ~50-fold, and ~2-fold increase in the antigen density to approximately 53 HA, 48 M1, and 156 M2 per influenza VLP, respectively. Taken together, this study represents a novel approach to enable the efficient incorporation of full-length M2 while enhancing both the yield and quality of influenza VLPs produced by Sf9 cells.

KEYWORDS: influenza virus-like particle (VLP), antigen density, universal influenza vaccine, M2, amantadine, Sf9 insect cells

nfluenza virus infection poses a significant global disease burden, causing an estimated three to five million cases of severe illness and 290 000-650 000 deaths each year worldwide. While vaccination has been successful in generating long-lasting immunity to many other viral infections, influenza vaccines must be updated and administered annually to match mutations that emerge in seasonal influenza strains and to boost antibody titers which begin to wane several months after vaccination.2 However, the long production timeline of the seasonal influenza vaccine (~6 months using the current eggbased method)3 often allows circulating strains to antigenically drift from the vaccine strains already in production. As a result, the current influenza vaccine efficacy in the U.S. fluctuates from 60% to as low as 10% for a given year.5 In addition to limited efficacy, seasonal influenza vaccines provide little protection against pandemic strains that arise from either interspecies transmission or reassortment of the influenza A hemagglutinin (HA) and neuraminidase (NA) subtypes through a process termed antigenic shift.<sup>6,7</sup> Given these limitations, new vaccine strategies that provide broader protection against mutation-prone seasonal influenza and potentially pandemic influenza are of great interest.8-11

One strategy for improving the efficacy of seasonal influenza vaccines is to develop new vaccines based on customizable

virus-like particles (VLPs). VLPs are commonly produced by recombinant expression of the influenza glycoproteins (i.e., HA and/or NA) and the matrix protein M1, which form budded particles that resemble the structure of the native influenza virus but lack the viral RNA. 12,13 In contrast to conventional influenza vaccines, VLPs can be produced rapidly (2-3 months) and be designed to include custom antigens with tunable surface densities. 13-18 Therefore, VLPs presenting broadly conserved influenza proteins have the potential to protect against both seasonal and pandemic influenza. 19 One of the best-studied and broadly conserved antigenic targets on influenza virus is the stalk domain of the HA protein.20 Although the HA stalk domain is largely conserved across HA subtypes,21 seasonal influenza infection or vaccination tends to elicit a much stronger (~100 000-fold) antibody response against the variable HA head domain, resulting in poor heterosubtypic protection. 22,23 Therefore, identifying additional broadly conserved influenza antigens capable of eliciting a robust antibody response is important for influenza vaccine development.

Received: March 15, 2019 Published: September 5, 2019



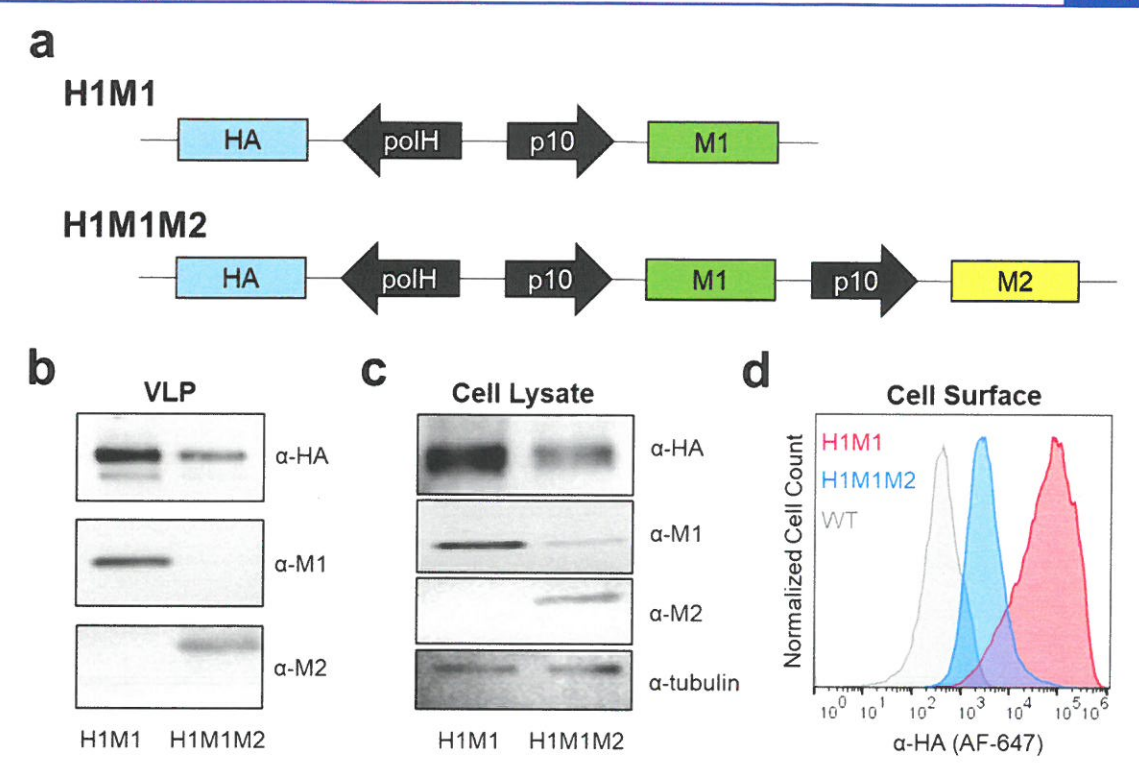


Figure 1. Characterizing the effects of M2 expression on influenza VLP production in Sf9 cells. (a) Schematic of the recombinant baculovirus vectors used to produce H1M1 and H1M1M2 influenza VLPs in Sf9 cells. Western blot analyses of influenza proteins in (b) purified VLPs and (c) baculovirus-infected cell lysates. Tubulin was used in (c) as a control to ensure equal amount of cell lysate was loaded for each sample. (d) Flow cytometric characterization of HA surface expression on H1M1- and H1M1M2-infected Sf9 cells at 72 hpi. WT baculovirus-infected cells were used as a negative control.

One promising antigenic target that has emerged in recent years is the influenza matrix protein M2.24 The M2 protein is highly conserved across all human influenza A subtypes, with ≥98% homology for the first 15 amino acids of the M2 ectodomain (M2e).25 However, antibody responses against M2e are generally absent following seasonal vaccination, which is likely a result of the low M2 antigen density (~16-20 M2 monomers/virus) and the immunodominance of the larger and more abundant HA (~1200 HA monomers/virus) and NA (~160 NA monomers/virus) proteins. 26-28 Significant efforts have been made to increase M2e surface density on influenza VLPs with the goal of eliciting a stronger M2e-specific antibody response.<sup>24</sup> To this end, a recent study demonstrated that fusing the M2e to a different transmembrane domain (e.g., HA) increases M2e surface density by >100-fold compared to native influenza virus.<sup>29</sup> Vaccination with these M2e VLPs resulted in improved M2e-specific antibody and T-cell responses, which led to reduced weight loss and higher survival rate of mice challenged with heterosubtypic influenza strains. 29,30

While M2e-fusion based VLPs have demonstrated great potential as a vaccine candidate, there are two significant advantages associated with incorporating full-length M2 into influenza VLPs. First, it is well-known that T cells are critical for heterosubtypic protection against influenza infection, especially when there is no preexisting antibody response due to antigenic drift or the emergence of a pandemic strain. The transmembrane and cytoplasmic domains of M2 contain T-cell epitopes that are capable of inducing long-lasting, broadly protective M2-specific CD4+ and CD8+ T-cell responses in mice. Many of these T-cell epitopes are even more conserved than those in the M2e across influenza A

subtypes of multiple species including human, swine and avian. <sup>34,35</sup> In addition, these epitopes are presented by HLA alleles A\*03:01, A\*11:01, and DRB1\*04:01 among others, <sup>36</sup> which are found in ~15–30% of Caucasians. <sup>37</sup> Therefore, new influenza vaccine designs incorporating full-length M2, as well as other highly conserved influenza internal proteins, <sup>38</sup> hold great promises for universal influenza vaccine development. <sup>39</sup> Second, the cytoplasmic tail of M2 is known to perform the membrane scission function, which facilitates influenza viral particle budding from host cells. <sup>40</sup> Therefore, incorporating full-length M2 into VLP-based influenza vaccines could improve VLP yield by promoting more efficient budding from the production host cell surface.

Insect cells are an attractive host for producing influenza VLPs due to their ability to express high levels of complex mammalian proteins; 15,41 however, the incorporation of fulllength M2 into influenza VLPs produced in insect cells is inadequate for vaccination purposes. In an early attempt to incorporate full-length M2 into influenza VLPs produced in Spodoptera frugiperda (Sf9) insect cells, M2 comprised only 1% of the total VLP proteins, 42 inducing substantially weaker Band T-cell responses compared to M2e-fusion based VLPs. 29,43 It has been shown in other host cells that the expression of fulllength M2 induces cytopathic effects, including rapid cell lysis in both E. coli44 and mammalian cells,45 as well as impaired growth rate of yeast. 46 While it has been suggested that M2 is also cytopathic when expressed in insect cells, 47 the nature and degree of these effects and how they affect influenza VLP production are largely unknown. In the present work, we quantitatively characterized the effects of full-length M2 expression on the production of influenza VLP as well as its protein components in Sf9 insect cells. Our data suggest that

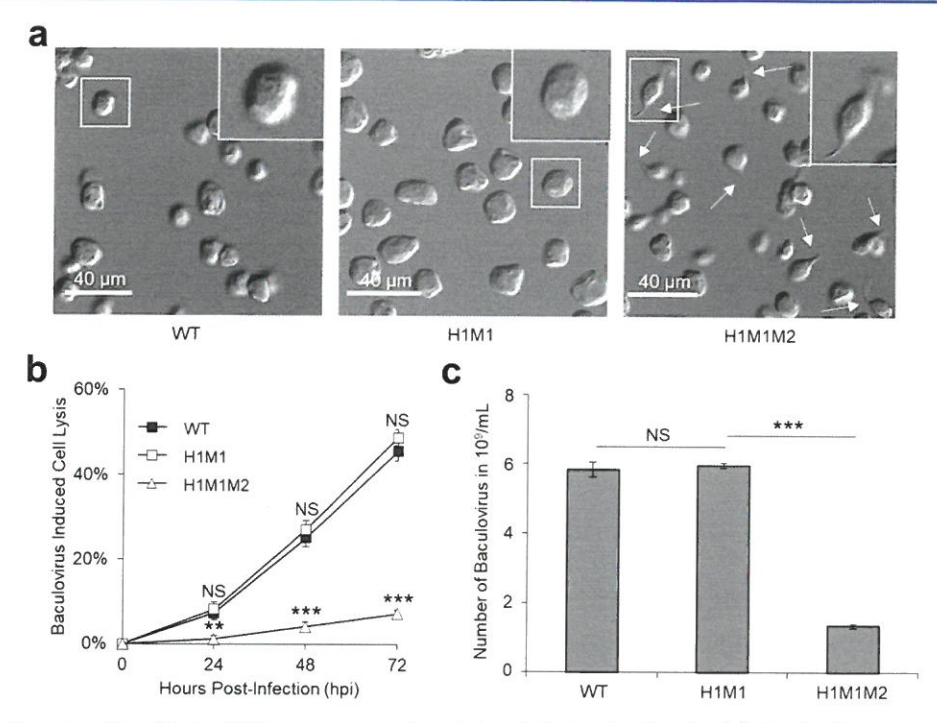


Figure 2. Quantifying the cytopathic effects of M2 expression on baculovirus infection in Sf9 cells. (a) Confocal microscopy images showing the morphology of WT, H1M1, and H1M1M2-infected Sf9 cells at 72 hpi. (b) Time course of baculovirus induced cell lysis. (c) Baculovirus titers (i.e., number of baculovirus in  $10^9$ /mL) in the supernatants of cells infected with indicated baculoviruses at 72 hpi. For (b) and (c), data represent mean  $\pm$  SE (n = 3, unpaired Student's t test, \*\*p < 0.01, \*\*\*p < 0.001, NS, p > 0.05, not significant).

the M2 ion channel activity induces significant cytopathic effects in Sf9 cells, resulting in impaired expression of not only M2, but also HA and M1 which are needed for influenza VLP production. We further demonstrate that the M2 ion channel inhibitor, amantadine, ameliorates the cytopathic effects of M2 and enhances both the yield and the quality (*i.e.*, antigen density) of influenza VLPs produced in Sf9 cells.

### RESULTS AND DISCUSSION

Characterizing the Effects of M2 Expression on Influenza VLP Production. To evaluate the effects of M2 expression on influenza VLP production in Sf9 cells, two baculovirus vectors were generated: one encoding HA and M1 (denoted H1M1) and the other encoding HA, M1, and M2 (denoted H1M1M2) (Figure 1a). All three genes were derived from the A/PR/8/34 (H1N1) influenza strain. Sf9 cells were subsequently infected with the resulting baculovirus vectors at a multiplicity of infection (MOI) of 3. At 72 h postinfection (hpi), influenza VLPs were purified from the supernatant (see Experimental Methods and ref 48) and analyzed by Western blots for influenza protein quantification. Influenza proteins produced in Sf9 cells showed expected antibody binding specificity and molecular weight in reference to purified HA (59 kDa), M1 (28 kDa), and M2 (15 kDa) protein standards (Figure S1). While the VLPs produced by H1M1M2-infected Sf9 cells contained M2, the amount of HA and M1 was significantly lower than that produced by H1M1-infected cells (Figure 1b). To determine if the decreased HA and M1 content in the H1M1M2 VLPs is due to reduced influenza protein expression in Sf9 cells, Western blot analysis of the cell lysates was performed. As shown in Figure 1c, the cellular expression levels of HA and M1 in H1M1M2-infected cells were significantly reduced compared to those of H1M1infected cells. We further performed flow cytometric analysis to

measure the HA expression level on the surface of infected Sf9 cells. H1M1-infected cells showed a strong increase in the median fluorescence intensity (MFI) relative to wild type baculovirus-infected cells (denoted WT) (Figure 1d). However, the MFI of H1M1M2-infected cells decreased ~10-fold compared to that of H1M1, indicating a similar reduction of HA expression on the cell surface (Figure 1d) to that in the cell lysate (Figure 1c). Taken together, these data suggest that the recombinant expression of full-length M2 in Sf9 cells impairs the expression of HA and M1 proteins, which are required for influenza VLP production.

Further, when observing the baculovirus infection in Sf9 cells during the production of influenza VLPs, the H1M1M2infected cells behaved differently than those infected with either WT or H1M1 baculovirus. The cells infected with the WT or H1M1 baculovirus displayed slightly enlarged and spherical morphologies that are typical of baculovirus infection (Figure 2a, WT and H1M1 panel). In contrast, ~50% of the H1M1M2-infected cells exhibited an elongated spindle morphology characterized by polar projections (Figure 2a, white arrows in H1M1M2 panel). Interestingly, this change in morphology for H1M1M2-infected cells was accompanied by a significant reduction in the rate of baculovirus-induced cell lysis: only ~7% of Sf9 cells had lysed by 72 hpi for H1M1M2infected cells compared to ~50% for either WT-infected or H1M1-infected cells (Figure 2b), despite that all infections were carried out at the same MOI of 3. As baculovirus infection ultimately results in cell lysis, the lack of cell lysis in the H1M1M2-infected cells suggests that the expression of M2 interferes with baculovirus replication. To test this hypothesis, we quantified the baculovirus titers (i.e., number of baculovirus in 109/mL) in these infected cell supernatants as described (see Experimental Methods and Figure S2). 49 Indeed, the baculovirus titer in the H1M1M2-infected cell supernatant was

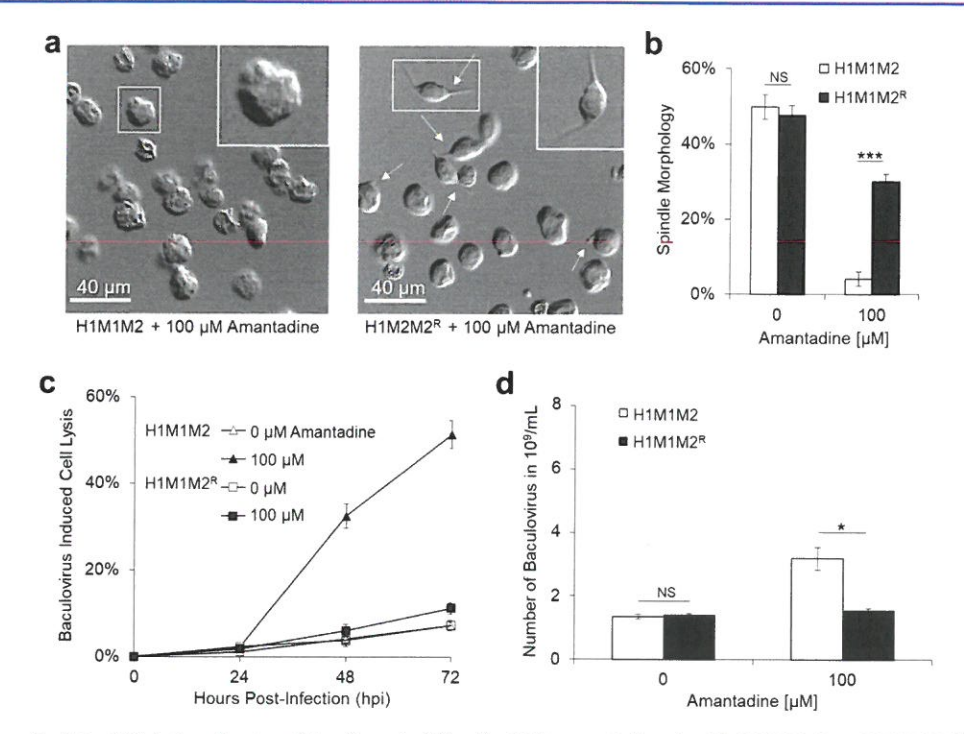


Figure 3. Amantadine alleviates M2-induced cytopathic effects in Sf9 cells. Cells were infected with H1M1M2 or H1M1M2<sup>R</sup> baculoviruses in the presence of 0 or 100  $\mu$ M amantadine as indicated. (a) Confocal microscopy images showing the morphology of H1M1M2- and H1M1M2<sup>R</sup> infected Sf9 cells. (b) Percentage of cells with spindle morphology at 72 hpi. (c) Time course of baculovirus induced cell lysis. (d) Baculovirus titers (i.e., number of baculovirus in  $10^9/\text{mL}$ ) in the supernatants of cells infected with indicated baculoviruses at 72 hpi. For (b) and (d), data represent mean  $\pm$  SE (n = 3, unpaired Student's t test, \*p < 0.05, \*\*\*\*p < 0.001, NS, p > 0.05, not significant).

reduced by >4-fold compared to that in the supernatant of cells infected with either WT or H1M1 baculovirus (Figure 2c).

Taken together, our data clearly demonstrate that M2 expression induces changes in the Sf9 cell morphology, delays baculovirus-induced cell lysis, and impairs baculovirus replication (Figure 2). These cytopathic effects further lead to significant reduction in recombinant influenza protein expression in Sf9 cells, impairing influenza VLP production (Figure 1). The cytopathic effects reported here are likely a direct result of the M2 ion channel activity, which has been shown to normalize the pH between the Golgi compartments and the cytoplasm in mammalian cell lines. 50 It is known that enzymes involved in protein synthesis and modification, such as ribosomes and glycosylation enzymes, are highly sensitive to pH.51,52 Therefore, it is likely that the ion channel activity of M2 causes pH perturbation in Sf9 cells outside of the normal operating range, which negatively impacts protein synthesis and modification. This negative impact may go beyond the influenza HA and M1 proteins as reported here to include others involved in baculovirus replication, lytic function, and Sf9 microtubule reorganization, which could explain the observed cytopathic effects and warrants future investigation.

Inhibiting M2 Ion Channel Activity Alleviates Cytopathic Effects in Sf9 Cells. Given the relationship between M2 ion channel activity and cytopathic effects in Sf9 cells, we next investigated if inhibiting the M2 ion channel activity can alleviate its cytopathic effects on Sf9 cells and enable the production of influenza VLPs with increased surface density of M2. Two strategies have been developed to inhibit M2 activity: mutagenesis and small molecule inhibition. Mutations in the transmembrane domain have been shown to either partially reduce or completely abolish M2 activity. The latter however would also abolish several highly conserved

T-cell epitopes for both human and mice.<sup>34</sup> We therefore chose to utilize amantadine, a small molecule that binds directly to the pore of the ion channel formed by the M2 tetramer and blocks proton translocation, to inhibit M2 ion channel activity.<sup>54</sup> Previous studies have shown that inhibiting M2 ion channel activity with amantadine can improve cellular expression of M2 in insect<sup>47</sup> and mammalian<sup>55</sup> cells. However, the effect of amantadine on the expression of other influenza proteins in insect cells and the production of influenza VLPs has not been explored. We hypothesized that the use of amantadine during baculovirus infection could alleviate the cytopathic effects induced by M2 expression. To test this hypothesis, a control is needed to separate the effects of ion channel inhibition from any potential extraneous effects of amantadine. To this end, a baculovirus vector (denoted H1M1M2<sup>R</sup>) was generated that was identical to the H1M1M2 vector except for two point mutations in the M2 protein (V27A, S31N). These two mutations confer amantadine resistance on the M2<sup>R</sup> protein with an IC<sub>50</sub> > 500  $\mu$ M, compared to the IC<sub>50</sub>  $\sim$  16  $\mu$ M for M2. 56,57

Next, the H1M1M2 and H1M1M2<sup>R</sup> baculoviruses were used to infect Sf9 cells at an MOI of 3 in the presence or absence of 100  $\mu$ M amantadine. The amantadine concentration of 100  $\mu$ M was chosen since it is well above the IC<sub>50</sub> of M2 and well below the IC<sub>50</sub> of M2<sup>R</sup>. In the absence of amantadine, H1M1M2<sup>R</sup>- and H1M1M2-infected cells behaved similarly, with ~50% cells exhibiting a spindle morphology (Figure 3b). In addition, both H1M1M2<sup>R</sup>- and H1M1M2-infected cells showed a reduced rate of cell lysis (Figure 3c), and impaired baculovirus replication (Figure 3d). However, when 100  $\mu$ M amantadine was added during the infection, <5% of H1M1M2-infected cells exhibited the spindle morphology compared to ~30% of H1M1M2<sup>R</sup>-infected cells

(Figure 3a,b). Thus, the use of  $100 \,\mu\text{M}$  amantadine was able to prevent the spindle morphology in the vast majority (>95%) of H1M1M2-infected cells, but not in H1M1M2<sup>R</sup>-infected cells.

Similar effects were observed when comparing the rate of baculovirus-induced cell lysis. The addition of 100  $\mu M$ amantadine to H1M1M2-infected cells restored the rate of lysis to a level comparable to that of WT- and H1M1-infected cells (Figures 3c and 2b), whereas the rate of H1M1M2Rinduced cell lysis remained largely unchanged (Figure 3c). Furthermore, H1M1M2 baculovirus titer was improved by >2fold, whereas the addition of 100 µM amantadine did not significantly improve the H1M1M2<sup>R</sup> baculovirus titer (Figure 3d). It should be noted that the use of 100  $\mu$ M amantadine did not restore the H1M1M2 baculovirus titer to the same level as that of WT or H1M1 (Figures 3d and 2c). It is possible that there may still be some residual cytopathic effect of M2 in the presence of 100  $\mu$ M amantadine. Alternatively, the ion channel activity of M2 may not be the sole mechanism accounting for the impaired baculovirus replication. Nevertheless, these data clearly demonstrate that the ion channel activity of M2 is indeed causing the aforementioned cytopathic effects in Sf9 cells, and these effects can be effectively alleviated by the use of amantadine during the baculovirus infection.

Amantadine Improves Cellular and Surface Expression of Influenza Proteins. After demonstrating that amantadine alleviates the cytopathic effects of M2 in Sf9 cells, we next investigated whether inhibiting M2 activity with amantadine improves the cellular expression of influenza proteins. Sf9 cells were infected with H1M1M2 baculovirus in the presence of varying concentrations of amantadine, and the cell lysates at 72 hpi were analyzed by Western blot. The cellular expression level of the three influenza proteins was then quantified using standard curves generated from purified HA, M1, and M2 protein (Figure S3). In the absence of amantadine, the cellular expression level of HA, M1, and M2 in H1M1M2-infected Sf9 cells was ~3, ~7, and ~8 mg/L, respectively (Figure 4a,b). In the presence of  $0.1-100 \mu M$ amantadine, the cellular expression level of each influenza protein increased in an amantadine-dose dependent manner, reaching a maximum of  $\sim$ 20,  $\sim$ 24, and  $\sim$ 28 mg/L at 100  $\mu$ M amantadine, for HA, M1, and M2, respectively (Figure 4a,b). Increasing the amantadine concentration to 1000 µM did not yield further improvement. The cellular expression level of HA observed in the presence of 100  $\mu$ M amantadine is within the commonly reported range for HA expression in Sf9 cells (20-30 mg/L).58 This suggests that HA expression in H1M1M2infected Sf9 cells can be restored by inhibiting M2 activity. Note that although the use of amantadine also restored baculovirus replication (Figure 3d), this increased baculovirus titer is unlikely the reason for the observed improvement of influenza protein cellular expression because Sf9 cells, once infected, become highly resistant to reinfection. 59 The MOI of 3 used in all the experiments ensured a minimal number (<5%) of uninfected Sf9 cells available for infection by the newly produced progeny baculoviruses. Interestingly, while the cellular expression level of each influenza protein was similarly high (20-28 mg/L) in the presence of 100  $\mu$ M amantadine, inhibiting M2 activity provided the greatest fold increase (~7fold) for HA cellular expression compared to ~3-fold increase for M1 and M2 (Figure 4c). This observation indicates that HA expression is more sensitive to M2 ion channel activity than both M1 and M2.

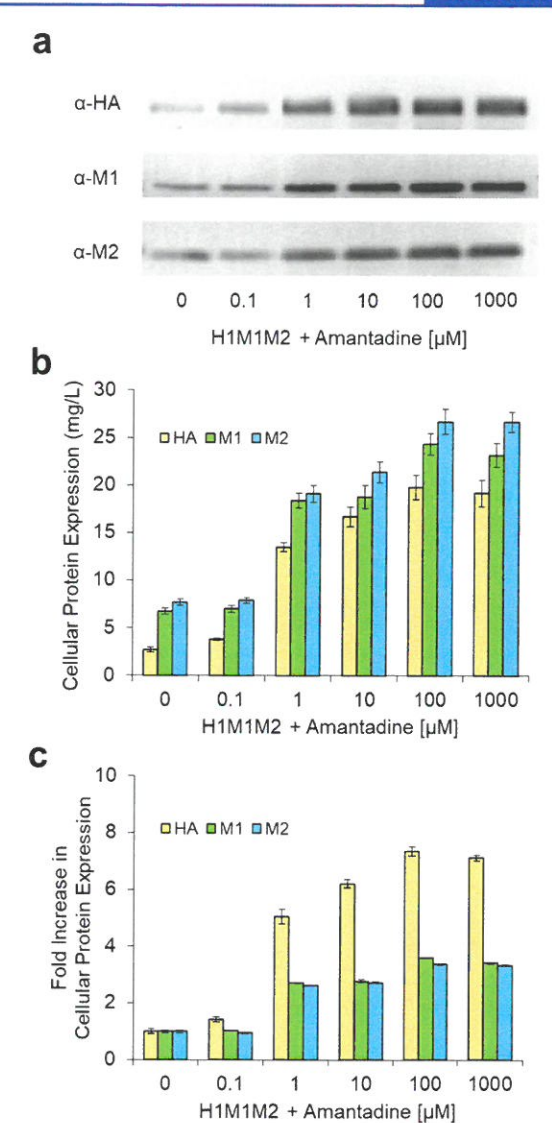


Figure 4. Amantadine improves the cellular expression of influenza proteins in Sf9 cells. The concentration of amantadine used in H1M1M2 infections is as indicated. (a) Western blot analysis of influenza proteins in H1M1M2-infected cell lysates at 72 hpi. (b) Cellular expression levels of influenza proteins. (c) Fold increase in cellular protein expression of each influenza protein relative to the value when no amantadine was used. For (b) and (c), data represent mean  $\pm$  SE (n=3).

Because influenza proteins must be at the host cell surface to be incorporated into VLPs, we next investigated the effect of amantadine on the surface expression of HA and M2 in Sf9 cells. At 72 hpi, H1M1M2-infected cells in the presence of varying concentrations of amantadine were surface costained with anti-HA and anti-M2 antibodies and analyzed by flow cytometry (see Experimental Methods). Uninfected Sf9 cells were used as a control to define the HA+ and M2+ cell populations (R2 gate, Figure 5a,b). An amantadine-dose dependent increase in the percentage of Sf9 cells expressing HA and M2 on the surface was observed, with both reaching a maximum of ~80% in the presence of  $\geq$ 10  $\mu$ M amantadine (Figure 5a,b). Further, the frequency of Sf9 cells coexpressing HA and M2 on the surface was also found to increase with amantadine concentration, reaching a maximum of ~67% at 100 µM amantadine (Figure 5c). These results indicate that

ACS Synthetic Biology

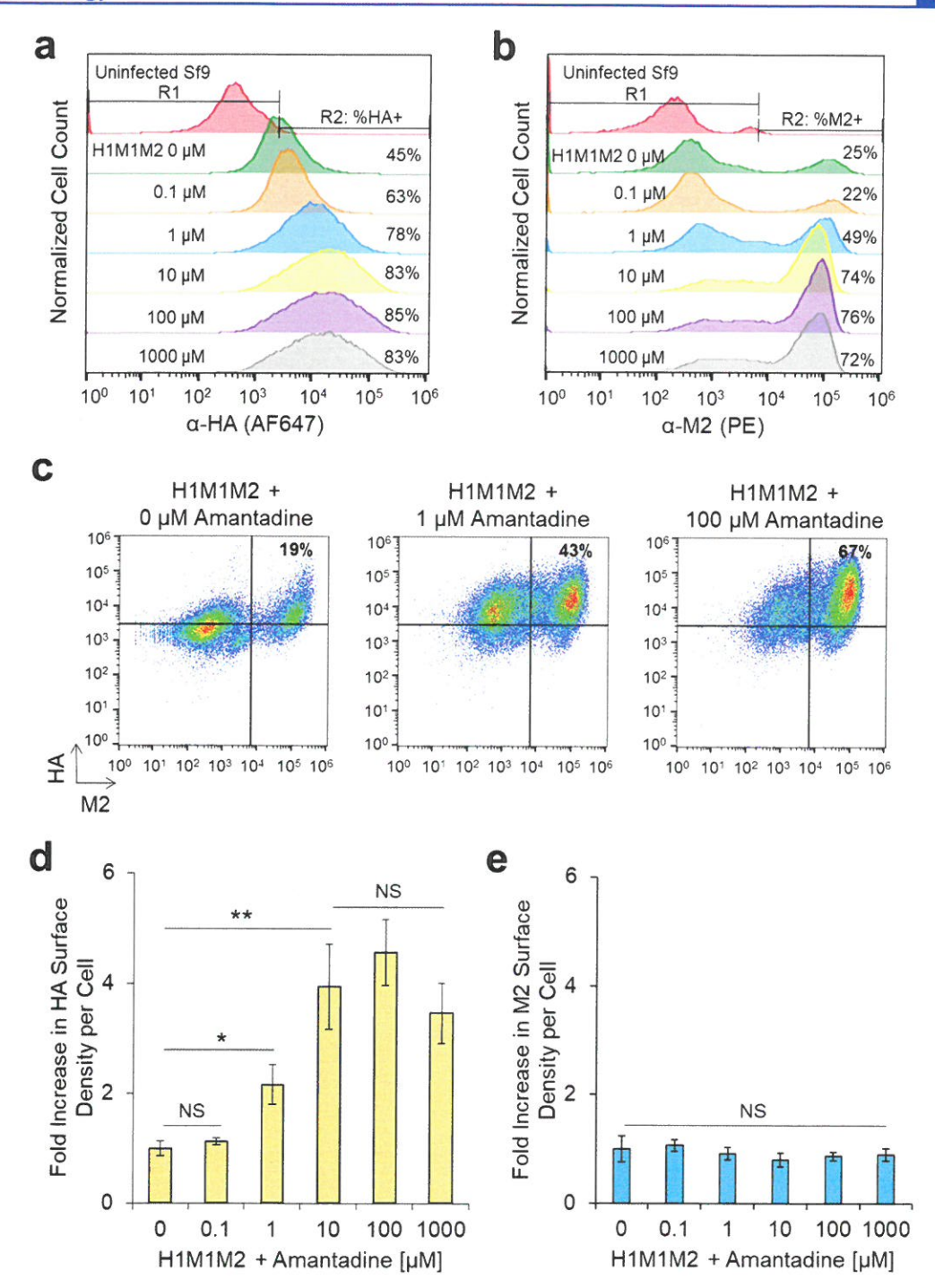
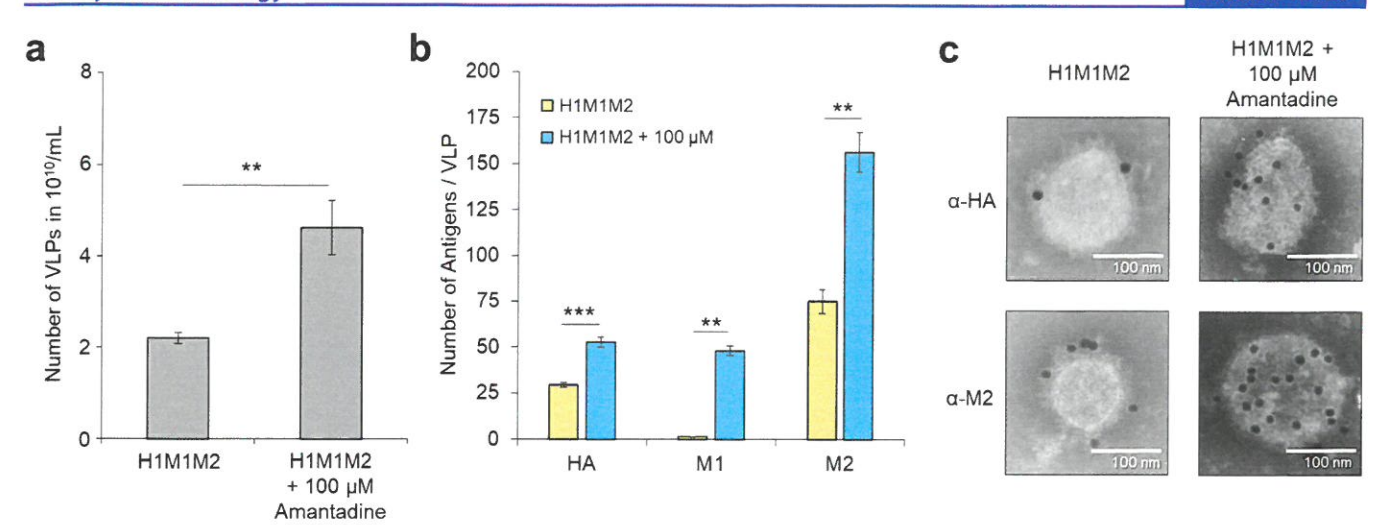


Figure 5. Amantadine improves the HA and M2 surface expression in Sf9 cells. The concentration of amantadine used in H1M1M2 infections is as indicated. Flow cytometric characterization of (a) HA and (b) M2 surface expression on H1M1M2-infected Sf9 cells at 72 hpi. Uninfected Sf9 cells (R1 gate, a and b) were used as a control for gating HA<sup>+</sup> (R2 gate, a) and M2<sup>+</sup> (R2 gate, b) cells. (c) Dot plots of HA vs M2 surface expression with the HA<sup>+</sup>M2<sup>+</sup> cell population frequency shown in the upper right quadrant of each plot. Fold increase in (d) HA and (e) M2 surface density per cell (i.e., MFI) for the HA<sup>+</sup>M2<sup>+</sup> cell population normalized to the value when no amantadine was used. For (d) and (e), data represent mean  $\pm$  SE (n = 3, unpaired Student's t test, \*p < 0.05, \*\*p < 0.01, NS, p > 0.05, not significant).

M2 activity limits the percentage of H1M1M2-infected Sf9 cells coexpressing the HA and M2 proteins on the surface. This observation may be partly attributed to the slower transport of both HA and M2 to the cell surface due to M2 activity as previously reported in mammalian cells, 50 though the precise underlying molecular mechanism requires further investigation. Nevertheless, the increased percentage of Sf9 cells coexpress-

ing influenza proteins on the surface is expected to increase influenza VLP yield.

While the percentage of HA<sup>+</sup>M2<sup>+</sup> Sf9 cells is expected to correlate with the yield of influenza VLPs, the HA and M2 surface density per Sf9 cell should in theory correlate with VLP quality (*i.e.*, antigen density per VLP). Therefore, we next evaluated the effect of amantadine on the HA and M2 surface density of the HA<sup>+</sup>M2<sup>+</sup> Sf9 cells by measuring their respective



**Figure 6.** Amantadine improves the yield and quality of influenza H1M1M2 VLPs in Sf9 cells. H1M1M2 VLPs were produced in the absence or presence of 100  $\mu$ M amantadine as indicated. (a) VLP yield reported as the number of VLPs per mL of cell culture. (b) VLP antigen density reported as the average number of influenza protein monomers per VLP. (c) Transmission electron microscopy (TEM) images showing HA (top) and M2 (bottom) immunogold labeled-VLPs. For (a) and (b), data represent mean  $\pm$  SE (n = 3, unpaired Student's t test, \*\*p < 0.01, \*\*\*p < 0.001).

MFI. When normalized by the MFI value obtained in the absence of amantadine, the HA surface density per cell showed an amantadine-dose dependent increase, reaching a maximum of  $\sim$ 5-fold improvement at  $\geq$ 10  $\mu$ M amantadine (Figure 5a,d). Surprisingly the M2 surface density per cell did not change significantly, regardless of the amantadine concentration used (Figure 5b,e). Combined with the results shown in Figure 4c, these data demonstrate that both the cellular and surface expression of HA in Sf9 cells is more sensitive to M2 ion channel activity than M2 itself. This greater sensitivity of HA could be potentially attributed to the fact that HA is a large membrane protein with 4-5 glycosylation sites. It is known that glycosylation is important for membrane protein folding, stability, and in many cases, transport from the Golgi to the cell surface. 60,61 Even minor changes in pH can impair the activity of glycosylation enzymes, 62 making HA more vulnerable to the M2-induced pH perturbation in the Golgi compartments.

Amantadine Improves Both Yield and Quality of **Influenza VLPs.** Because the use of 100  $\mu$ M amantadine resulted in both maximum cellular expression of all three influenza proteins (Figure 4) and maximum percentage of HA+M2+ Sf9 cells (Figure 5c), we next aimed to evaluate if it leads to greater influenza VLP yield and quality. The number of influenza VLPs purified from H1M1M2-infected Sf9 cell supernatant at 72 hpi in the presence or absence of 100  $\mu$ M amantadine was quantified using nanoparticle tracking analysis (NTA) (see Experimental Methods). As expected, the use of 100  $\mu$ M amantadine indeed increased the yield of the influenza VLPs by  $\sim$ 2-fold (Figure 6a), which is in line with the  $\sim$ 3-fold increase in the percentage of HA+M2+ Sf9 cells (Figure 5c). Since it is well-known that influenza proteins can also pseudotype into baculovirus, 63 we evaluated the extent of baculovirus contamination in the VLP sample as detailed in Figure S4. Consistent with the data in Figure 3d, the number of baculovirus increased by ~2-fold in the presence of amantadine; however, baculoviruses only accounted for ~5% of the total particles in the VLP sample (Figure S4). Combined with the fact that all infections were conducted at an MOI of 3 and Sf9 cells are highly resistant to reinfection, 59 these data suggest that the improvement in VLP yield is driven by the

increased influenza protein expression in the presence of amantadine and not by secondary infection of the newly produced baculoviruses.

To measure the antigen density of influenza VLPs, the amount of HA, M1, and M2 in the VLPs was quantified by Western blot using purified HA, M1, and M2 proteins as standard (Figure S5). The antigen density in these VLPs was then calculated as the number of each influenza protein monomer divided by the number of VLPs. As shown in Figure 6b, the influenza VLPs produced in the absence of amantadine had an antigen density of ~29 HA/VLP, ~1 M1/VLP, and  $\sim$ 75 M2/VLP. The use of 100  $\mu M$  amantadine resulted in greater antigen density of all three influenza proteins: ~53 HA/VLP, ~48 M1/VLP, and ~156 M2/VLP, representing a ~2-fold, ~50-fold, and ~2-fold improvement, respectively. This improvement in VLP antigen density was further confirmed by visualizing HA and M2 immunogold-labeled VLPs using transmission electron microscopy (TEM). As shown in Figure 6c, the influenza VLPs produced from Sf9 cells showed morphology resembling that of influenza virus with spike-like projections and a diameter between 80 and 200 nm. Influenza VLPs produced in the presence of 100  $\mu$ M amantadine showed a greater degree of HA and M2 immunogold labeling than those produced without amantadine, which is consistent with the greater VLP antigen density reported above.

Unexpectedly, when we compared the fold increase of HA and M2 surface density per Sf9 cell (Figure 5d,e) with the fold increase of HA and M2 density per VLP (Figure 6b) in the presence of 100  $\mu$ M amantadine, the data suggest that these two parameters are actually not well correlated: 5-  $\nu$ s 2-fold for HA and 0-  $\nu$ s 2-fold for M2. More strikingly, while the use of 100  $\mu$ M amantadine only improved the M1 cellular expression by ~3-fold (Figure 4c), it resulted in a ~50-fold increase in the M1 density per VLP (Figure 6b). Therefore, the cellular and/or surface expression level of influenza proteins does not determine how efficiently they are incorporated into VLPs. Instead, it is well-known that influenza protein—protein interactions and their association with the plasma membrane are critical for driving the budding of VLPs.  $^{64-67}$  For example,

M1 is known to oligomerize at the inner leaflet of the plasma membrane, which both strengthens its association with HA contained in lipid rafts and induces bending of the plasma membrane to initiate particle budding. Coincidentally, oligomerization of M1 is also pH-dependent; under low pH conditions, M1 undergoes a conformational change that releases itself from the plasma membrane back into the cytosol. Therefore, restoring the normal intracellular pH by inhibiting M2 activity with amantadine likely allows M1 to better associate with HA at the plasma membrane and thus results in its efficient incorporation into VLPs.

Over the past two decades, the frequency of influenza viruses with the wild type M2 used in this study has diminished to <2% of circulating strains as of 2015, while amantadineresistant M2 variants increased to >98%.71,72 These amantadine-resistant M2 variants have similar IC50 values as the M2R protein studied here. Therefore, we also quantified the effect of amantadine on influenza protein expression and VLP production for H1M1M2R in Sf9 cells. Compared to H1M1M2, similar improvements in cellular expression of all three influenza proteins (Figure S6), HA and M2<sup>R</sup> surface expression (Figure S7), VLP yield and antigen density (Figure S8) were achieved for H1M1M2<sup>R</sup>, albeit at a much higher concentration of amantadine (2500 µM). These data demonstrate that a sufficiently high concentration of amantadine can also alleviate the cytopathic effects of M2R ion channel activity and improve the yield and quality of VLPs for vaccine designs toward current circulating influenza strains.

Significant effort has been made to develop vaccines that provide broadly protective, long-lasting immunity against influenza infection. While the M2 matrix protein has emerged as an attractive vaccination target due to its highly conserved sequence, its expression has been associated with cytopathic effects in recombinant host cells, making it challenging to produce influenza VLPs with high surface density of full-length M2. Here we show for the first time that inhibiting M2 activity with amantadine leads to improved influenza VLP production in Sf9 insect cells showing both greater yield and higher antigen density. The H1M1M2 VLPs produced in the presence of 100  $\mu$ M amantadine display 8–10-fold higher density of M2 on their surface compared to influenza virus, which may stimulate both stronger and broader M2-specific B- and T-cell responses. However, the HA density of these VLPs (~55 HA monomers/VLP) is much lower than that of influenza virus (~1200 HA monomers/virus). As a result, the H1M1M2 VLPs reported here show a drastically inverted ratio of HA:M2 (1:3) compared to influenza virus (>10:1). Given the fact that the current influenza vaccines (i.e., inactivated influenza virus) suffer from poor heterosubtypic protection due to the immunodominant responses to the HA head domain, these H1M1M2 VLPs may prove advantageous in promoting a more balanced immune response for a broader protection. Taken together, these results present a promising outlook for the vaccination potential of these engineered influenza VLPs with high density of full-length M2 as a heterosubtypic vaccine candidate.

### **EXPERIMENTAL METHODS**

Strains, Media, and Reagents. Sf9 insect cells (CRL-1711, ATCC, Manassas, VA) were grown in Insect XPRESS Media (Lonza, Walkersville, MD) supplemented with 10 mg/L gentamycin at 27 °C and 135 rpm agitation. Madin—Darby Canine Kidney (MDCK) cells (a kind gift from Dr. Malini

Raghavan, University of Michigan, Ann Arbor) were grown in Dulbecco's Modified Eagle Media (DMEM) supplemented with 10% fetal calf serum (FCS), 100 U/mL penicillin and 100 µg/mL streptomycin. DH10Bac cells (Bac-to-Bac Baculovirus Expression Systems, Life Technologies, Foster City, CA) were grown in Luria-Bertani (LB) medium containing 50 µg/mL kanamycin, 7  $\mu$ g/mL gentamicin and 10  $\mu$ g/mL tetracycline. Influenza virus strain A/Puerto Rico/8/1934 (PR8) (VR-1469, ATCC) was propagated in MDCK cells at 37 °C and 5% CO<sub>3</sub>. PR8 viral RNA was extracted using the ZR Viral RNA Kit (Zymo Research, Irvine, CA) and reverse transcribed into complementary DNA (cDNA) using the Transcriptor First Strand cDNA Synthesis kit (Roche, Penzberg, Germany) according to the manufacturers' protocols. Unless otherwise stated, all media and antibiotics were purchased from Thermo Fisher Scientific (Waltham, MA) and all other chemicals were purchased from Sigma-Aldrich (St. Louis, MO). All primers were purchased from Integrated DNA Technologies (Coralville, IA).

Recombinant Baculovirus Generation. DNA sequences encoding the HA and M1 genes were amplified from the viral cDNA by polymerase chain reaction (PCR) and cloned into the XbaI/HindIII and KpnI/XmaI site in plasmid pFastBac Dual, respectively, to create plasmid pFastBac Dual-H1M1. The templates and primers used for all PCR reactions are listed in Table S1. The DNA sequence encoding the M2R gene was PCR amplified from the PR8 viral cDNA and cloned into the XhoI/XmaI site of pFastBac Dual to create plasmid pFastBac Dual-M2<sup>R</sup>. The wild type M2 gene was then generated by introducing two mutations (A27V, N31S) into pFastBac Dual-M2<sup>R</sup> using overlap extension PCR. Specifically, two fragments (M2-F1 and M2-F2 in Table S1) were spliced and cloned into the XhoI/XmaI site of pFastBac Dual to create pFastBac Dual-M2. The expression cassette for M2<sup>R</sup> (or M2) including the P10 promoter, M2<sup>R</sup> (or M2) gene, and HSV terminator was then PCR amplified from pFastBac Dual-M2R (or M2) and cloned into the AvrII site of pFastBac Dual-H1M1 to create pFastBac Dual-H1M1M2<sup>R</sup> (or pFastBac Dual-H1M1M2). All DNA sequences were confirmed using Sanger sequencing.

The recombinant baculovirus genome (i.e., bacmid) was created by transforming plasmid pFastBac Dual-H1M1, pFastBac Dual-H1M1M2, or pFastBac Dual-H1M1M2<sup>R</sup> into DH10Bac via transposition. The empty pFastBac Dual plasmid was treated similarly to generate the "WT" baculovirus as a control. After confirming the recombination events by blue/white colony screening and PCR, the recombinant bacmids were purified using a PureLink HiPure Plasmid Miniprep kit (Invitrogen, Carlsbad, CA). The purified bacmids were then transfected into Sf9 cells using Cellfectin II (Invitrogen) according to manufacturer's protocol to generate recombinant baculovirus P1 stocks, which were amplified in Sf9 cells to obtain high-titer P2 baculovirus stocks for use in protein expression experiments.

**Baculovirus Titer Determination.** Baculovirus titers of P2 stocks were quantified using a flow cytometric assay <sup>49</sup> with slight modification. Briefly, 2 mL of Sf9 cells seeded at a density of  $2.0 \times 10^6$  cells/mL were infected with 2-fold serial dilutions of the P2 stock in a six-well plate. At 24 hpi, cells were stained with 2 ng/ $\mu$ L anti-GP64 PE antibody (BioLegend, San Diego, CA) for 1 h at room temperature prior to analysis using an Attune Acoustic Focusing Cytometer (Applied Biosystems, Foster City, CA). Uninfected Sf9 cells were used as a control for gating GP64+ cells. The percentage

of GP64<sup>+</sup> cells was used to calculate the multiplicity of infection (MOI) using the equation below simplified from the inverse Poisson distribution.<sup>73</sup>

MOI 
$$\equiv \frac{\text{number of baculovirus}}{\text{number of cells}} = -\ln\left(\frac{100 - \text{\%GP64}^+}{100}\right)$$

Given that  $4.0 \times 10^6$  cells were used in each well, the baculovirus titer in each of the six wells can then be calculated as  $4.0 \times 10^6 \times \text{MOI}$  divided by the volume of P2 stock used. To increase the accuracy of the calculated baculovirus titer, the values of  $4.0 \times 10^6 \times \text{MOI}$  were plotted with respect to the volume of P2 stock used for each of the six wells, and the slope of the resulting linear regression was determined to be the baculovirus titer (Figure S2).

Sf9 Cell Infection Characterization and Influenza Protein Quantification. Baculovirus-infected Sf9 cell morphology was visually assessed at 72 hpi using a Leica TCS SP8MP inverted confocal microscope (Nikon, Melville, NY), and the number of cells with spindle morphology was counted using a hemocytometer (Hausser Scientific, Horsham, PA). For each baculovirus construct, a total of at least 100 cells from triplicate infections were analyzed. The amount of baculovirus-induced cell lysis was similarly quantified as the percentage of dead cells at 24, 48, and 72 hpi using Trypan blue staining and a hemocytometer.

Cellular expression of HA, M1, and M2 protein was quantified by Western blot analysis of cell lysates using purified HA (BEI Resources, Manassas, VA), M1 (Sino Biological, Beijing, China) and M2 (purified from *E. coli* as described)<sup>74</sup> as protein standards. Antibodies used include anti-HA (Sino Biological), anti-M1 (Invitrogen), and anti-M2 (Invitrogen) antibodies, alkaline phosphatase-conjugated antimouse or antirabbit IgG secondary antibody (Life Technologies), and antitubulin antibody (BioLegend). All antibodies were used at a working concentration of 0.3 ng/ $\mu$ L. Densitometric analysis of Western blots was performed using a Gel Doc EZ Imager (Bio-Rad, Hercules, CA) to generate standard curves for HA, M1, and M2 (Figure S3), which were then used to calculate their cellular expression level.

The surface expression of HA and M2 on infected Sf9 cells was quantified by flow cytometric analysis. Specifically, at 72 hpi cells were costained with anti-HA and anti-M2 antibodies, followed by secondary staining with antirabbit biotin antibody (Life Technologies) and then tertiary costaining with antimouse IgG Alexa Fluor 647 antibody (AF647, BioLegend) and Streptavidin PE (eBiosciences, San Diego, CA) prior to analysis on the Attune Acoustic Focusing Cytometer. All antibodies were used at a working concentration of 2 ng/ $\mu$ L. Uninfected Sf9 cells were treated the same way and used as a control for gating.

Virus-like Particle (VLP) Production and Characterization. Influenza VLPs were produced from Sf9 cells infected at an MOI of 3 and harvested 72 hpi. Cell debris was removed from the supernatant by centrifugation at 300g for 20 min followed by 10 000g for 20 min. The cleared supernatant was overlaid on a 30% sucrose sublayer and centrifuged at 150 000g for 2 h, and the pellet containing VLPs was resuspended in PBS + 40% glycerol. All centrifugation steps were carried out at 4 °C.

The number of VLPs was quantified using a NanoSight NS300 particle tracking system (Malvern Panalytical, Malvern, United Kingdom). Specifically, VLPs were diluted in PBS to

manufacturer recommended concentrations prior to injection. Videos of 60 s were recorded for three injections of each sample, and the particle concentration was determined using the nanoparticle tracking analysis (NTA) software provided with the NS300 system. The amount of HA, M1, and M2 in each VLP preparation was quantified by densitometric analysis of Western blots as described in the section above.

VLPs were visually characterized by immunogold-labeling analysis using transmission electron microscopy (TEM). Briefly, VLPs were absorbed on Ni grids (Electron Microscopy Sciences, Hatfield, PA) and incubated with 20 ng/ $\mu$ L anti-HA or anti-M2 antibody for 1 h, followed by labeling with protein G–gold nanoparticle (15 nm) conjugates (Electron Microscopy Sciences) at a concentration of  $10^{11}$  gold nanoparticles/mL for 30 min. Grids were stained with 2% phosphotungstic acid (PTA) and allowed to dry 1 h prior to TEM analysis on a JEM-1400 Transmission Electron Microscope, 80 kV (JEOL, Peabody, MA).

**Statistical Analysis.** Statistical analysis was performed using unpaired Student's t test. All data are represented as the mean of three independent experiments and error bars represent the standard error of mean (SE). \*p < 0.05, \*\*p < 0.01, \*\*\*p < 0.001, not significant (NS) p > 0.05.

#### ASSOCIATED CONTENT

## Supporting Information

The Supporting Information is available free of charge on the ACS Publications website at DOI: 10.1021/acssynbio.9b00111.

Baculovirus vector construction (Table S1), influenza protein identification, baculovirus titer quantification, baculovirus contamination quantification, cellular and VLP protein standard curve generation, H1M1M2<sup>R</sup> cellular and surface expression quantification, H1M1M2<sup>R</sup> VLP yield and antigen density (Figures S1–S8) (PDF)

# AUTHOR INFORMATION

## **Corresponding Author**

\*E-mail: feiwenum@umich.edu.

ORCID ©

Fei Wen: 0000-0001-7970-4796

#### **Author Contributions**

FW conceived and supervised the project. AJZ, BDH, and FW designed the experiments. AJZ, BDH, SMR, and MY performed the experiments. BDH, FW, AJZ, and MRS analyzed the data and wrote the manuscript. All authors read and revised the manuscript.

#### Notes

The authors declare no competing financial interest.

# ACKNOWLEDGMENTS

The authors thank all group members from Dr. Fei Wen's lab for their constructive feedback. The authors also thank the University of Michigan Microscopy and Image Analysis Laboratory (MIL) for assistance with TEM. This work was supported by the National Science Foundation (NSF) CAREER Award 1653611, grants 1511720 and 1645229, the National Institute of Health (NIH) grant OD020053, and the MCubed program at the University of Michigan. FW and SMR

were additionally supported by the Rogel Cancer Center Support Grant (NIH P30 CA046592).

#### REFERENCES

- (1) WHO (2018) Influenza (Seasonal), World Health Organization, Geneva. https://www.who.int/news-room/fact-sheets/detail/influenza-(seasonal), accessed February 3, 2019.
- (2) Ferdinands, J. M., Fry, A. M., Reynolds, S., Petrie, J., Flannery, B., Jackson, M. L., and Belongia, E. A. (2016) Intraseason waning of influenza vaccine protection: Evidence from the US Influenza Vaccine Effectiveness Network, 2011–12 through 2014–15. *Clin. Infect. Dis.* 64, 544–550.
- (3) Manini, I., Trombetta, C. M., Lazzeri, G., Pozzi, T., Rossi, S., and Montomoli, E. (2017) Egg-Independent Influenza Vaccines and Vaccine Candidates. *Vaccines* 5, 18.
- (4) Osterholm, M. T., Kelley, N. S., Sommer, A., and Belongia, E. A. (2012) Efficacy and effectiveness of influenza vaccines: a systematic review and meta-analysis. *Lancet Infect. Dis.* 12, 36–44.
- (5) CDC Presents Updated Estimates of Flu Vaccine Effectiveness for the 2014–2015 Season | News (Flu), Center for Disease Control. https://www.cdc.gov/flu/vaccines-work/effectiveness-studies.htm, accessed February 3, 2019.
- (6) Neumann, G., Noda, T., and Kawaoka, Y. (2009) Emergence and pandemic potential of swine-origin H1N1 influenza virus. *Nature* 459, 931–939.
- (7) Skowronski, D. M., De Serres, G., Crowcroft, N. S., Janjua, N. Z., Boulianne, N., Hottes, T. S., Rosella, L. C., Dickinson, J. A., Gilca, R., Sethi, P., Ouhoummane, N., Willison, D. J., Rouleau, I., Petric, M., Fonseca, K., Drews, S. J., Rebbapragada, A., Charest, H., Hamelin, M.-E., Boivin, G., Gardy, J. L., Li, Y., Kwindt, T. L., Patrick, D. M., Brunham, R. C., and Canadian SAVOIR Team, for the C. S. (2010) Association between the 2008–09 seasonal influenza vaccine and pandemic H1N1 illness during Spring-Summer 2009: four observational studies from Canada. *PLoS Med.* 7, e1000258.
- (8) Kumar, A., Meldgaard, T. S., and Bertholet, S. (2018) Novel Platforms for the Development of a Universal Influenza Vaccine. Front. Immunol. 9, 600.
- (9) Huang, M., Huang, W., Wen, F., and Larson, R. G. (2017) Efficient estimation of binding free energies between peptides and an MHC class II molecule using coarse-grained molecular dynamics simulations with a weighted histogram analysis method. *J. Comput. Chem.* 38, 2007–2019.
- (10) Wen, F., Rubin-Pitel, S. B., and Zhao, H. (2009) Engineering of Therapeutic Proteins, In *Protein Engineering and Design* (Park, S. J., and Cochran, J. R., Eds.), pp 153–177, CRC Press.
- (11) Ross, K. A., Huntimer, L. M., Vela Ramirez, J. E., Adams, J. R., Carpenter, S. L., Kohut, M. L., Bronich, T., Webby, R., Legge, K. L., Mallapragada, S. K., Wannemuehler, M. J., and Narasimhan, B. (2014) Vaccine Technologies Against Avian Influenza: Current Approaches and New Directions. J. Biomed. Nanotechnol. 10, 2261–2294.
- (12) Wong, S.-S., and Webby, R. J. (2013) Traditional and new influenza vaccines. Clin. Microbiol. Rev. 26, 476–492.
- (13) Fuenmayor, J., Gòdia, F., and Cervera, L. (2017) Production of virus-like particles for vaccines. *New Biotechnol.* 39, 174–180.
- (14) Hill, B. D., Zak, A., Khera, E., and Wen, F. (2017) Engineering Virus-like Particles for Antigen and Drug Delivery. *Curr. Protein Pept. Sci.* 19, 112–127.
- (15) Yee, C. M., Zak, A. J., Hill, B. D., and Wen, F. (2018) The Coming Age of Insect Cells for Manufacturing and Development of Protein Therapeutics. *Ind. Eng. Chem. Res.* 57, 10061–10070.
- (16) Fernandes, F., Teixeira, A. P., Carinhas, N., Carrondo, M. J., and Alves, P. M. (2013) Insect cells as a production platform of complex virus-like particles. *Expert Rev. Vaccines* 12, 225–236.
- (17) Smith, M. R., Tolbert, S. V., and Wen, F. (2018) Protein-Scaffold Directed Nanoscale Assembly of T Cell Ligands: Artificial Antigen Presentation with Defined Valency, Density, and Ratio. ACS Synth. Biol. 7, 1629–1639.

(18) Raeeszadeh-Sarmazdeh, M., Hartzell, E., Price, J. V., and Chen, W. (2016) Protein nanoparticles as multifunctional biocatalysts and health assessment sensors. *Curr. Opin. Chem. Eng.* 13, 109–118.

- (19) Quan, F.-S., Lee, Y.-T., Kim, K.-H., Kim, M.-C., and Kang, S.-M. (2016) Progress in developing virus-like particle influenza vaccines. *Expert Rev. Vaccines* 15, 1281–1293.
- (20) Lu, Y., Welsh, J. P., and Swartz, J. R. (2014) Production and stabilization of the trimeric influenza hemagglutinin stem domain for potentially broadly protective influenza vaccines. *Proc. Natl. Acad. Sci. U. S. A. 111*, 125–130.
- (21) Kirkpatrick, E., Qiu, X., Wilson, P. C., Bahl, J., and Krammer, F. (2018) The influenza virus hemagglutinin head evolves faster than the stalk domain. *Sci. Rep. 8*, 10432.
- (22) Sui, J., Sheehan, J., Hwang, W. C., Bankston, L. A., Burchett, S. K., Huang, C.-Y., Liddington, R. C., Beigel, J. H., and Marasco, W. A. (2011) Wide Prevalence of Heterosubtypic Broadly Neutralizing Human Anti-Influenza A Antibodies. *Clin. Infect. Dis.* 52, 1003–1009.
- (23) Klausberger, M., Tscheliessnig, R., Neff, S., Nachbagauer, R., Wohlbold, T. J., Wilde, M., Palmberger, D., Krammer, F., Jungbauer, A., and Grabherr, R. (2016) Globular Head-Displayed Conserved Influenza H1 Hemagglutinin Stalk Epitopes Confer Protection against Heterologous H1N1 Virus. *PLoS One* 11, e0153579.
- (24) Kolpe, A., Schepens, B., Fiers, W., and Saelens, X. (2017) M2-based influenza vaccines: recent advances and clinical potential. *Expert Rev. Vaccines* 16, 123–136.
- (25) Fiers, W., De Filette, M., Birkett, A., Neirynck, S., and Min Jou, W. (2004) A "universal" human influenza A vaccine. *Virus Res.* 103, 173–176.
- (26) Nayak, D. P., Hui, E. K.-W., and Barman, S. (2004) Assembly and budding of influenza virus. *Virus Res.* 106, 147–165.
- (27) Samji, T. (2009) Influenza A: understanding the viral life cycle. *Yale J. Biol. Med.* 82, 153–159.
- (28) Altman, M. O., Angeletti, D., and Yewdell, J. W. (2018) Antibody Immunodominance: The Key to Understanding Influenza Virus Antigenic Drift. *Viral Immunol.* 31, 142–149.
- (29) Kim, M.-C., Song, J.-M., Eunju, O., Kwon, Y.-M., Lee, Y.-J., Compans, R. W., and Kang, S.-M. (2013) Virus-like Particles Containing Multiple M2 Extracellular Domains Confer Improved Cross-protection Against Various Subtypes of Influenza Virus. *Mol. Ther.* 21, 485–492.
- (30) Kim, Y.-J., Lee, Y.-T., Kim, M.-C., Lee, Y.-N., Kim, K.-H., Ko, E.-J., Song, J.-M., and Kang, S.-M. (2017) Cross-Protective Efficacy of Influenza Virus M2e Containing Virus-Like Particles Is Superior to Hemagglutinin Vaccines and Variable Depending on the Genetic Backgrounds of Mice. Front. Immunol. 8, 1730.
- (31) Sridhar, S., Begom, S., Bermingham, A., Hoschler, K., Adamson, W., Carman, W., Bean, T., Barclay, W., Deeks, J. J., and Lalvani, A. (2013) Cellular immune correlates of protection against symptomatic pandemic influenza. *Nat. Med.* 19, 1305–1312.
- (32) Clemens, E., van de Sandt, C., Wong, S., Wakim, L., and Valkenburg, S. (2018) Harnessing the Power of T Cells: The Promising Hope for a Universal Influenza Vaccine. *Vaccines* 6, 18.
- (33) Wilkinson, T. M., Li, C. K. F., Chui, C. S. C., Huang, A. K. Y., Perkins, M., Liebner, J. C., Lambkin-Williams, R., Gilbert, A., Oxford, J., Nicholas, B., Staples, K. J., Dong, T., Douek, D. C., McMichael, A. J., and Xu, X.-N. (2012) Preexisting influenza-specific CD4+ T cells correlate with disease protection against influenza challenge in humans. *Nat. Med.* 18, 274–280.
- (34) Tutykhina, I., Esmagambetov, I., Bagaev, A., Pichugin, A., Lysenko, A., Shcherbinin, D., Sedova, E., Logunov, D., Shmarov, M., Ataullakhanov, R., Naroditsky, B., and Gintsburg, A. (2018) Vaccination potential of B and T epitope-enriched NP and M2 against Influenza A viruses from different clades and hosts. *PLoS One* 13, e0191574.
- (35) Muñoz-Medina, J. E., Sánchez-Vallejo, C. J., Méndez-Tenorio, A., Monroy-Muñoz, I. E., Angeles-Martínez, J., Santos Coy-Arechavaleta, A., Santacruz-Tinoco, C. E., González-Ibarra, J., Anguiano-Hernández, Y.-M., González-Bonilla, C. R., Ramón-Gallegos, E., and Díaz-Quiñonez, J. A. (2015) In Silico Identification

of Highly Conserved Epitopes of Influenza A H1N1, H2N2, H3N2, and H5N1 with Diagnostic and Vaccination Potential. *BioMed Res. Int.* 2015, 813047.

- (36) Kim, Y., Ponomarenko, J., Zhu, Z., Tamang, D., Wang, P., Greenbaum, J., Lundegaard, C., Sette, A., Lund, O., Bourne, P. E., Nielsen, M., and Peters, B. (2012) Immune epitope database analysis resource. *Nucleic Acids Res.* 40, W525–530.
- (37) González-Galarza, F. F., Takeshita, L. Y. C., Santos, E. J. M., Kempson, F., Maia, M. H. T., Silva, A. L. S. da, Silva, A. L. T. e, Ghattaoraya, G. S., Alfirevic, A., Jones, A. R., and Middleton, D. (2015) Allele frequency net 2015 update: new features for HLA epitopes, KIR and disease and HLA adverse drug reaction associations. *Nucleic Acids Res.* 43, D784–D788.
- (38) Terajima, M., Babon, J., Co, M., and Ennis, F. A. (2013) Cross-reactive human B cell and T cell epitopes between influenza A and B viruses. *Virol. J.* 10, 244.
- (39) Nachbagauer, R., and Krammer, F. (2017) Universal influenza virus vaccines and therapeutic antibodies. *Clin. Microbiol. Infect.* 23, 222–228.
- (40) Rossman, J. S., Jing, X., Leser, G. P., and Lamb, R. A. (2010) Influenza virus M2 protein mediates ESCRT-independent membrane scission. *Cell* 142, 902–913.
- (41) Geisler, C., Mabashi-Asazuma, H., and Jarvis, D. L. (2015) *Methods Mol. Biol.* 1321, 131–152.
- (42) Song, J.-M., Wang, B.-Z., Park, K.-M., Van Rooijen, N., Quan, F.-S., Kim, M.-C., Jin, H.-T., Pekosz, A., Compans, R. W., and Kang, S.-M. (2011) Influenza Virus-Like Particles Containing M2 Induce Broadly Cross Protective Immunity. *PLoS One* 6, e14538.
- (43) Kim, M.-C., Lee, J.-S., Kwon, Y.-M., O, E., Lee, Y.-J., Choi, J.-G., Wang, B.-Z., Compans, R. W., and Kang, S.-M. (2013) Multiple heterologous M2 extracellular domains presented on virus-like particles confer broader and stronger M2 immunity than live influenza A virus infection. *Antiviral Res.* 99, 328–335.
- (44) Guinea, R., and Carrasco, L. (1994) Influenza virus M2 protein modifies membrane permeability in E. coli cells. *FEBS Lett.* 343, 242–246.
- (45) Ilyinskii, P. O., Gabai, V. L., Sunyaev, S. R., Thoidis, G., and Shneider, A. M. (2007) Toxicity of Influenza A Virus Matrix Protein 2 for Mammalian Cells is Associated with its Intrinsic Proton-Channeling Activity. *Cell Cycle* 6, 2043–2047.
- (46) Kurtz, S., Luo, G., Hahnenberger, K. M., Brooks, C., Gecha, O., Ingalls, K., Numata, K., and Krystal, M. (1995) Growth impairment resulting from expression of influenza virus M2 protein in Saccharomyces cerevisiae: identification of a novel inhibitor of influenza virus. *Antimicrob. Agents Chemother.* 39, 2204–2209.
- (47) Black, R. A., Rota, P. A., Gorodkova, N., Cramer, A., Klenk, H.-D., and Kendal, A. P. (1993) Production of the M2 protein of influenza A virus in insect cells is enhanced in the presence of amantadine. *J. Gen. Virol.* 74, 1673–1677.
- (48) Arevalo, M. T., Wong, T. M., and Ross, T. M. (2016) Expression and Purification of Virus-like Particles for Vaccination. *J. Visualized Exp.*, 54041.
- (49) Mulvania, T., Hayes, B., and Hedin, D. (2004) Vol 3, No 3 (2004) A Flow Cytometric Assay for Rapid, Accurate Determination of Baculovirus Titers. *BioProcess. J. 3*, 47–53.
- (50) Henkel, J. R., and Weisz, O. A. (1998) Influenza virus M2 protein slows traffic along the secretory pathway. pH perturbation of acidified compartments affects early Golgi transport steps. J. Biol. Chem. 273, 6518–6524.
- (51) Rivinoja, A., Pujol, F. M., Hassinen, A., and Kellokumpu, S. (2012) Golgi pH, its regulation and roles in human disease. *Ann. Med.* 44, 542–554.
- (52) Johansson, M., Ieong, K.-W., Trobro, S., Strazewski, P., Åqvist, J., Pavlov, M. Y., and Ehrenberg, M. (2011) pH-sensitivity of the ribosomal peptidyl transfer reaction dependent on the identity of the A-site aminoacyl-tRNA. *Proc. Natl. Acad. Sci. U. S. A. 108*, 79–84.
- (53) Balannik, V., Carnevale, V., Fiorin, G., Levine, B. G., Lamb, R. A., Klein, M. L., DeGrado, W. F., and Pinto, L. H. (2010) Functional

Studies and Modeling of Pore-Lining Residue Mutants of the Influenza A Virus M2 Ion Channel. *Biochemistry* 49, 696-708.

- (54) Kozakov, D., Chuang, G.-Y., Beglov, D., and Vajda, S. (2010) Where does amantadine bind to the influenza virus M2 proton channel? *Trends Biochem. Sci.* 35, 471–475.
- (55) Sakaguchi, T., Leser, G. P., and Lamb, R. A. (1996) The ion channel activity of the influenza virus M2 protein affects transport through the Golgi apparatus. *J. Cell Biol.* 133, 733–747.
- (56) Rey-Carrizo, M., Torres, E., Ma, C., Barniol-Xicota, M., Wang, J., Wu, Y., Naesens, L., DeGrado, W. F., Lamb, R. A., Pinto, L. H., and Vazquez, S. (2013) 3-Azatetracyclo[5.2.1.1<sup>5,8</sup>.0<sup>1.5</sup>]undecane Derivatives: From Wild-Type Inhibitors of the M2 Ion Channel of Influenza A Virus to Derivatives with Potent Activity against the V27A Mutant. *J. Med. Chem.* 56, 9265–9274.
- (57) Wang, J., Wu, Y., Ma, C., Fiorin, G., Wang, J., Pinto, L. H., Lamb, R. A., Klein, M. L., and Degrado, W. F. (2013) Structure and inhibition of the drug-resistant S31N mutant of the M2 ion channel of influenza A virus. *Proc. Natl. Acad. Sci. U. S. A. 110*, 1315–1320.
- (58) Margine, I., Palese, P., and Krammer, F. (2013) Expression of functional recombinant hemagglutinin and neuraminidase proteins from the novel H7N9 influenza virus using the baculovirus expression system. *J. Visualized Exp.*, e51112.
- (59) Gotoh, T., Ando, N., and Kikuchi, K.-I. (2008) Re-Infection Profile of Baculoviruses to Sf-9 Insect Cells that Have Already Been Infected: Virus Binding and Recombinant Protein Production. J. Chem. Eng. Jpn. 41, 804–808.
- (60) Scheiffele, P., and Füllekrug, J. (2000) Glycosylation and protein transport. *Essays Biochem.* 36, 27–35.
- (61) Watanabe, I., Zhu, J., Recio-Pinto, E., and Thornhill, W. B. (2015) The Degree of N-glycosylation Affects the Trafficking and Cell Surface Expression Levels of Kv1.4 Potassium Channels. J. Membr. Biol. 248, 187–196.
- (62) Reynders, E., Foulquier, F., Annaert, W., and Matthijs, G. (2011) How Golgi glycosylation meets and needs trafficking: the case of the COG complex. *Glycobiology* 21, 853–863.
- (63) Yang, D.-G., Chung, Y.-C., Lai, Y.-K., Lai, C.-W., Liu, H.-J., and Hu, Y.-C. (2007) Avian Influenza Virus Hemagglutinin Display on Baculovirus Envelope: Cytoplasmic Domain Affects Virus Properties and Vaccine Potential. *Mol. Ther.* 15, 989–996.
- (64) Veit, M., and Thaa, B. (2011) Association of influenza virus proteins with membrane rafts. *Adv. Virol.* 2011, 370606.
- (65) Leser, G. P., and Lamb, R. A. (2017) Lateral Organization of Influenza Virus Proteins in the Budozone Region of the Plasma Membrane. *J. Virol.* 91, e02104-02116.
- (66) Chen, B. J., Leser, G. P., Jackson, D., and Lamb, R. A. (2008) The influenza virus M2 protein cytoplasmic tail interacts with the M1 protein and influences virus assembly at the site of virus budding. *J. Virol.* 82, 10059–10070.
- (67) Rossman, J. S., and Lamb, R. A. (2011) Influenza virus assembly and budding. *Virology* 411, 229-236.
- (68) Zhang, K., Wang, Z., Fan, G.-Z., Wang, J., Gao, S., Li, Y., Sun, L., Yin, C.-C., and Liu, W.-J. (2015) Two polar residues within C-terminal domain of M1 are critical for the formation of influenza A Virions. *Cell. Microbiol.* 17, 1583–1593.
- (69) Li, S., Sieben, C., Ludwig, K., Höfer, C. T., Chiantia, S., Herrmann, A., Eghiaian, F., and Schaap, I. A. T. (2014) pH-Controlled Two-Step Uncoating of Influenza Virus. *Biophys. J.* 106, 1447–1456.
- (70) Fontana, J., and Steven, A. C. (2013) At low pH, influenza virus matrix protein M1 undergoes a conformational change prior to dissociating from the membrane. *J. Virol.* 87, 5621–5628.
- (71) Dong, G., Peng, C., Luo, J., Wang, C., Han, L., Wu, B., Ji, G., and He, H. (2015) Adamantane-Resistant Influenza A Viruses in the World (1902–2013): Frequency and Distribution of M2 Gene Mutations. *PLoS One* 10, e0119115.
- (72) Durrant, M. G., Eggett, D. L., and Busath, D. D. (2015) Investigation of a recent rise of dual amantadine-resistance mutations in the influenza A M2 sequence. *BMC Genet.* 16, S3.

(73) Figliozzi, R. W., Chen, F., Chi, A., and Hsia, S.-C. V. (2016) Using the inverse Poisson distribution to calculate multiplicity of infection and viral replication by a high-throughput fluorescent imaging system. *Virol. Sin.* 31, 180–183.

(74) Alavi-Esfahani, M., Fotouhi-Chahooki, F., Saleh, M., Tavakoli, R., Farahmand, B., Ghaemi, A., and Tavassoti-Kheiri, M. (2012) Over Expression of Influenza Virus M2 Protein in Prokaryotic System. *Iran. J. Virol. 6*, 13–19.

2314

DOI: 10.1021/acssynbio.9b00111